Journal of Structural Geology 33 (2011) 624–632

Contents lists available at ScienceDirect

Journal of Structural Geology

journal homepage: www.elsevier.com/locate/jsg

Microstructure and mechanical properties of halite/coarse muscovite synthetic aggregates deformed in torsion

F.O. Marques*[,1], L. Burlini, J.-P. Burg

Department of Geosciences, Swiss Federal Institute of Technology (ETH-Zürich), CH-8092 Zurich, Switzerland

ARTICLE INFO

Article history:
Received 9 April 2010
Received in revised form
23 December 2010
Accepted 8 January 2011
Available online 15 January 2011

Keywords:
Torsion experiments
Two-phase aggregate
Halite (rock salt)
Muscovite kink
Mica-fish
Rheology with polymer jackets
Quartz/muscovite mylonite

ABSTRACT

We investigated the behavior of a synthetic two-phase aggregate composed of 80% halite + 20% coarse muscovite under torsion deformation, at 100, 200 and 300 °C, a confining pressure of 250 MPa, and a constant strain rate of 3E−4 s^{-1}. At all temperatures, the two-phase aggregate deformed homogeneously at the sample scale. The strength of the aggregate and muscovite deformation depended on temperature, strain rate and initial orientation of muscovite greatest dimension relative to the shear plane. With muscovite initially parallel to the shear plane, halite flowed plastically and long muscovite grains were not strong enough to behave as a rigid inclusion rotating in a ductile matrix. Instead, high aspect ratio grains deformed by folding, which was visibly accomplished by slip along mica {001} cleavage and by great flattening of halite in the core of the folds. When initially normal to the shear plane, high aspect ratio muscovite grains passively rotated towards the shear plane. In both cases, small and low aspect ratio muscovite grains behaved mostly as mica-fish, with mica grains tilted opposite to shear sense. Similarly to natural mylonites, σ-porphyroclast systems and rolling structures were also common in the microstructure. A strong foliation made of halite ribbons and aligned muscovite flakes rapidly developed but did not make the composite aggregate weaker when compared with single-phase halite. Comparison with synthetic aggregates of single-phase halite shows that the two-phase aggregate was much stronger than single-phase halite in all cases. Comparison with a synthetic aggregate with calcite porphyroclasts shows that the strength of the aggregate with muscovite at 100 °C was lower below a strain of ca. 2.6 and higher beyond this value, and that the aggregate with calcite was stronger at 200 °C. Strain rate stepping tests (1E−5 s^{-1}–2E−3 s^{-1}) indicate that the two-phase aggregate behaved as power-law viscous, with stress exponents of ca. 12 and 10 at 100 and 200 °C, respectively. The mechanical data obtained in this study represent the actual rheological behavior of the aggregates because we used soft polymer jackets.

1. Introduction

Deforming rocks exhibit, at all scales, complex rheological responses ranging from strong quasi-rigid-like to weak quasi-fluid-like effective behavior, as a function of temperature, stress, strain rate, fluids and/or rock composition. In many cases, both behaviors are found in the same deformed rock as, for example, in porphyritic granites deformed in greenschist facies conditions, where “hard” feldspar porphyroclasts are immersed in a “soft” plastically deformed (fine grained) matrix of quartz and mica, or quartz–mica rocks where quartz is the fluid-like phase and mica is the rigid-like phase. Handy (1990) suggested that the mechanical and microstructural behavior of such polymineralic rocks can be described by three end-member types: (1) strong minerals form a load-bearing framework; (2) two or more minerals with low relative strengths control bulk rheology; (3) one very weak mineral governs bulk rheology, while the stronger minerals form porphyroclasts. The samples we used in the present work fall on type 3; however, the experimental results presented here indicate that 20% of unconnected mica porphyroclasts can influence the bulk rheology of the aggregate, and that this influence grows with temperature. This is still an open and relevant question because the solid-state rheology of rocks depends to a great extent on the relative proportions of weak and strong minerals, their shape and orientation, and distribution. Therefore, we also tested the effect of mineral shape and orientation (angle between greatest mica dimension and shear plane), and crystal lattice type on bulk rheology. We also compare

* Corresponding author. Universidade Lisboa and IDL, 1749-016 Lisboa, Portugal. Tel.: +41 44 6328918; fax: +41 44 6321030.
E-mail addresses: fomarques@fc.ul.pt, fernando.ornelas@erdw.ethz.ch (F.O. Marques).
[1] Deceased. Most of this article had been written when L. Burlini died on 22.12.2009.

0191-8141/$ – see front matter © 2011 Elsevier Ltd. All rights reserved.
doi:10.1016/j.jsg.2011.01.003

the present experiments using platy porphyroclasts with previous experiments carried out under similar conditions but with more equant calcite grains as porphyroclasts (Marques et al., 2010a).

The use of mixed strong and weak phases poses a practical problem for experimental approaches, because in the laboratory most common natural ductile matrices (calcite or quartz) do not deform plastically at temperatures typical of the greenschist facies, very common to many ductile shear zones involving the plastic deformation of calcite and quartz. In trying to overcome this problem, we used as analogues (as did e.g. Williams et al., 1977; Hobbs et al., 1982) a soft (at low temperature and laboratory strain rates) plastic matrix made of halite, with immersed coarse grain muscovite clasts, to investigate the behavior and mechanical properties of a two-phase porphyritic synthetic aggregate with contrasting rheology and behavior of the constituents. In order to assess the influence of coarse muscovite on the bulk rheology of the composite aggregate, we compare it with the experimental behavior of synthetic single-phase halite aggregates deformed under similar experimental conditions.

To our knowledge, most low temperature work with two-phase aggregates has been done in axial compression and low strain. However, a great deal of deformation of rocks takes place in ductile shear zones dominated by simple shear (e.g. Ramsay, 1967). It is thus very advantageous to make available microstructural and mechanical data resulting from simple shear deformation to large strains. In particular, the natural behavior of muscovite within a weaker ductile matrix (commonly quartz or halite) under simple shear is still not well understood. Neither is the rheological influence of muscovite in the overall behavior of the aggregate when associated with weaker mineral phases. With this aim, we carried out torsion experiments to simulate strain in shear zones and achieve the high shear strains typical of natural mylonites.

The investigation of the rotational behavior of rigid inclusions is also relevant for the study and characterization of ductile shear zones, under variable conditions of flow, inclusion aspect ratio, inclusion/matrix contact (slip or no-slip) and inclusion/channel ratio (confinement)(e.g. Marques et al., 2007 and references therein). Therefore, the present experiments also aimed at investigating the rotational behavior of coarse muscovite in a ductile halite matrix. The determination of the amount of porphyroclast rotation under simple shear is problematic as theoretically discussed by Marques and Coelho (2003), and so is here investigated experimentally. Because we used torsion, we can also compare foliation development under rotational and irrotational strain. The use of a soft matrix with immersed platy minerals also permits investigation of the influence that the initial orientation of the mica plates may have on mica internal deformation, on microstructure and on bulk rheology; therefore, we used samples with muscovite at different initial angles with the applied shear.

Previous experimental work has used two-phase aggregates to analyze the effect of randomly distributed hard grains on the mechanics of the composite: halite/calcite (e.g. Jordan, 1987; Bloomfield and Covey-Crump, 1993; Kawamoto and Shimamoto, 1998; Marques et al., 2010a), halite/anhydrite (e.g. Price, 1982; Ross et al., 1987), calcite/quartz (e.g. Dresen and Evans, 1993; Dresen et al., 1998; Rybacki et al., 2003; Renner et al., 2007), anorthite/quartz (Xiao et al., 2002), calcite/anhydrite (Bruhn and Casey, 1997; Bruhn et al., 1999; Barnhoorn et al., 2005), calcite/muscovite (e.g. Delle Piane et al., 2009), or to gain a better understanding of mylonites (e.g. Ross et al., 1987; Jordan, 1987), or to study foliation development in quartz–mica rocks (e.g. Williams et al., 1977; Hobbs et al., 1982; Wilson, 1983; Burg and Wilson, 1987) or slates (Kanagawa, 1991). The results of the present experiments broadly agree with previous experimental work, but significant differences will be discussed below. Some of the differences may be related to the fact that we used a porphyritic aggregate, contrary to previous work with two-phase aggregates where both constituents had similar grain size.

The samples were subjected to torsion in an internally heated Paterson-type triaxial deformation apparatus. We did not investigate the deformation mechanisms of halite in torsion for two main reasons: (i) it was done previously at the ETH-Zürich (Armann, 2008; Wenk et al., 2009), and (ii) we did not manage to polish the samples conveniently for EBSD because hard muscovite grains get loose during polishing and deeply scratch the surface. However, we analyzed the microstructure and evaluated the mechanical properties of the composite aggregate.

When we wanted to determine the mechanical properties of the aggregates, we did not use metal jackets because, as shown by Marques et al. (2010b), the metal jackets mask the actual strength of the aggregates. Therefore we used polymer jackets to obtain mechanical data free of the metal jacket mechanical and chemical influences.

2. Materials and methods

2.1. Sample preparation

The specimens were synthesized by cold pressing a mixture of 80% halite (analytical grade powder with grain size <500 μm) and 20% of muscovite (average grain size >500 μm). This volume fraction was chosen in order to represent common porphyritic rocks where phenocrysts do not interact during deformation. Some quartz grains existed in the aggregate because the mica batch was not pure muscovite. Pressing produced a preferred alignment of muscovite grains roughly perpendicular to the maximum compressive stress (Fig. 1a). The synthetic aggregate was then hot isostatically stored at 200 °C for one week. Cold pressing and halite annealing were responsible for the gentle folding/kinking of some thin and elongated muscovite grains observed in the starting material (Fig. 1a). Microscopic analysis shows that the contact between halite grains was marked by muscovite dust (mostly) and fluid inclusions, which made visible the stretched individual halite grains after deformation. Cylindrical samples 15 mm in diameter were cored and oven-dried at 110 °C and atmospheric pressure for at least 24 h before the tests. Because halite is soluble in water, drilling was made with compressed air and polishing was carried out dry. Two types of samples were drilled, depending on the angle φ between the shear plane and the initial muscovite foliation: $\varphi = 0°$ and $\varphi = 90°$. The samples were inserted in a 0.5 mm thick and 15 mm inner diameter polymer jacket to assess the mechanical properties of the aggregate. In order to try and reach higher shear strain at 200 and 300 °C, we occasionally used copper jackets, but only for the microstructural analysis.

2.2. Deformation apparatus and boundary conditions

The experiments were conducted in a Paterson rig based on a standard gas-medium, high-pressure and high-temperature triaxial deformation machine, to which an additional module has been added that allows rotary shear of a cylindrical specimen (Paterson and Olgaard, 2000). In torsion experiments, near simple shear deformation occurs locally at any given position in the sample. The shear strain γ and shear strain rate $\dot{\gamma}$ increase linearly from zero along the central axis of the sample to a maximum value at the outer circumference. The $\dot{\gamma}$ at any radius can be calculated from the angular displacement rate using Eq. (3) in Paterson and Olgaard (2000). The experimental γ and $\dot{\gamma}$ mentioned are therefore the maximum values. The temperature distributions were regularly calibrated so that the temperature variation across the

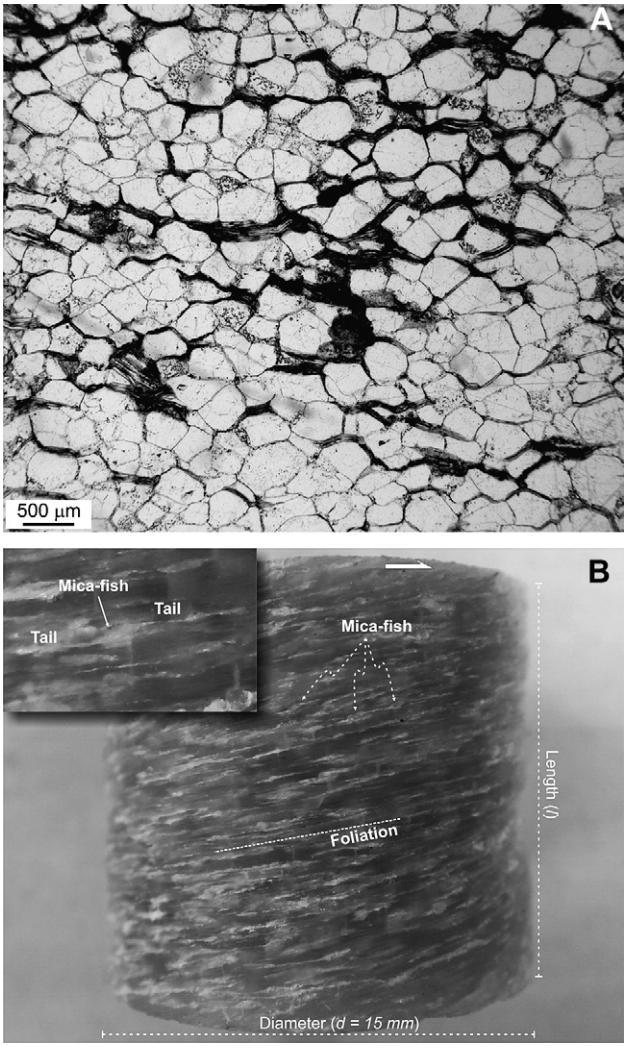

Fig. 1. Image of the overall aspect of starting material (A, transmitted light micrograph image) and image of sample deformed to $\gamma \approx 5.5$ at 100 °C (B, surface of the sample cylinder). A – long and thin muscovite grains conform to the halite grains (open folding), and muscovite roughly align to make an initial foliation. B – Note the homogeneous character of deformation. Inset is a zoom to show a mica-fish with tails made of small mica grains disrupted from the main grain. Stair stepping agrees with the applied sense of shear (top to right).

sample was never more than ±1 °C. The experiments were conducted at 100, 200 and 300 °C, at 250 MPa confining pressure and at constant angular displacement rate corresponding to a $\dot{\gamma} \approx 3E{-}4\ s^{-1}$, up to $\gamma \approx 6$. The runs for the 300 °C experiment were carried out using copper jackets because polymer jackets do not hold for long-term experiments. Therefore, only the microstructure is shown for the 300 °C experiment.

Strain rate stepping (SRS) tests ($\dot{\gamma}$ from $1E{-}5\ s^{-1}$ to $2E{-}3\ s^{-1}$) were run to determine the dependence of flow strength on $\dot{\gamma}$. The response of the internal torque M to a variation in angular displacement rate ($\dot{\theta}$) yields the stress exponent n ($n = \Delta \ln \dot{\theta} / \Delta \ln M$) (Eq. (12) of Paterson and Olgaard, 2000), which can give an indication of the active deformation mechanism.

3. Experimental results

3.1. Torque-twist data

Curves of torque vs. torsion strain (Fig. 2) were constructed to evaluate the response of the samples, in terms of resistance to flow (torque), to an applied constant twist rate. At 100 °C, all curves show an early fast loading to a yield followed by strain hardening. When $\varphi = 0°$, the curve for the composite aggregate with muscovite shows a step in torque around 1.5–1.7, which is preceded by transient steady-state flow. Above $\gamma \approx 2.6$, the $\varphi = 0°$ aggregate was the strongest. Zooming on the very early stages of loading (Fig. 2b) shows a gradual transition from the elastic to the plastic behavior. Comparison of the present results with previous experiments, under similar conditions and 100 °C, with one-phase halite and two-phase aggregates with 70% halite + 30% calcite (Marques et al., 2010a) shows that: (i) the single-phase halite aggregate was the weakest. (ii) The curve for single-phase halite also shows the step in torque following a transient constant flow torque. (iii) The two-phase aggregate with calcite was the strongest until $\gamma \approx 2.6$; beyond this point, the aggregate with muscovite was the strongest. (iv) The single-phase halite was the only aggregate showing a clear yield (Fig. 2b). The slope of the early linear curves differed among samples, being highest for the two-phase aggregate with calcite and lowest for the single-phase halite.

In all samples at 200 °C (Fig. 2c and d), yield was followed by steep hardening till about $\gamma \approx 0.5$. After this stage, the two-phase aggregates underwent gentle hardening, although a bit steeper for the $\varphi = 90°$ aggregate. Comparison of the present results with previous experiments, under similar conditions and 200 °C, with one-phase halite and two-phase aggregates with 70% halite + 30% calcite (Marques et al., 2010b) shows that the single-phase halite aggregate was by far the weakest, which flowed steadily below 10 MPa after $\gamma \approx 0.5$, and that the two-phase aggregate with calcite was the strongest.

The stress may be related to strain rate (SRS data) by either an exponential or a power law; however, the best fit is the power-law curve, which is shown in Fig. 3. From the best fit equations, stress exponents $n \approx 12$ and $n \approx 10$ were determined for 100 and 200 °C, respectively.

3.2. Microstructure

Despite the 20 volume% of muscovite in the aggregate, the experiments were characterized by homogeneous deformation at the sample scale (Fig. 1b), and at all tested temperatures. At the grain scale, however, deformation was heterogeneous and occasionally localized in ductile micro shear bands. Halite grains deformed plastically and homogeneously away from, and plastically but heterogeneously around muscovite clasts. Muscovite behavior depended on aspect ratio and initial orientation: (1) $\varphi = 0°$ – muscovite folded (Figs. 4, 5 and 6), or stabilized (at least transiently) dipping opposite to shear sense (typical of mica-fish), or slipped along {001} planes, or fractured; (2) $\varphi = 90°$ – muscovite stretched and all initial kinks were flattened, and many mica-fish formed (Fig. 4). At high strain (Figs. 4, 5a,b and 6b) most mica grains seemed to have attained a stable or transient metastable orientation at low angle to the shear foliation. At high strain a strong foliation formed that was made of halite ribbons and aligned muscovite flakes. At lower strain many muscovite grains could be observed at high angle to the shear plane, indicating synthetic rotation of thick, rigid mica grains toward the shear plane (Figs. 5c,d and 6a). Quartz grains typically showed signs of rotation (Figs. 4, 6 and 7). Fracturing of quartz grains was most likely inherited from cold pressing.

The microstructures experimentally produced were very similar at all temperatures, and find their counterparts in natural mylonites (Fig. 8) (e.g. Lister and Price, 1978; Berthé et al., 1979; Burg et al., 1981; Choukroune et al., 1987; Gaudemer and Tapponnier, 1987; Marques et al., 2007). This is the case of: (i) Mica-fish (Lister and Snoke, 1984) – between $\gamma = 3$ and 5 a strong foliation had formed by alignment of halite ribbons and muscovite flakes; many

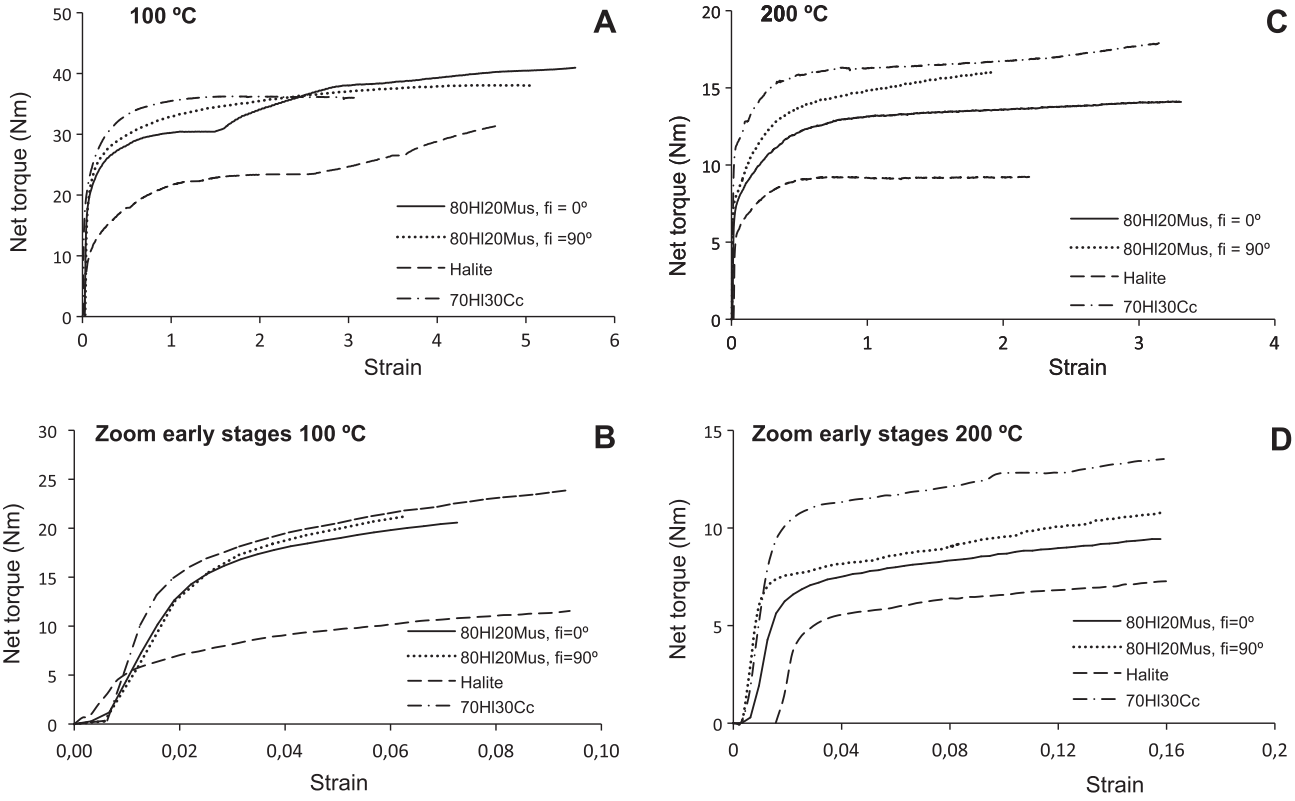

Fig. 2. Torque/strain curves for the two-phase aggregate with coarse muscovite at 100 (A and B) and 200 °C (C and D). Also in the graphs and for comparison are the curves for single-phase halite and two-phase aggregate with halite and calcite. The addition of coarse calcite or muscovite to halite significantly increased the strength of the aggregate. A – Note similarity of shape of the curves for single-phase halite and composite aggregate with muscovite. Also note that, at high strain, the composite aggregate with muscovite was the strongest. B – The plastic yield is sharper for the single-phase halite aggregate, and the slope of the initial straight varies among samples; it is highest for the composite aggregate with calcite and lowest for the single-phase halite aggregate. C – Note that all curves at 200° C show strain hardening (although gentle) till the end of the run, except for single-phase halite. Also note that the composite aggregate with calcite was the strongest, and that the aggregate with muscovite with initial $\varphi = 0°$ was the weakest. D – At 200 °C, the plastic yield is sharper for all samples when compared to the experiments at 100 °C; the slope of the initial straight is highest for the composite aggregates with calcite and muscovite with initial $\varphi = 90°$.

of these looked like the mica-fish described in the literature (e.g. ten Grotenhuis et al., 2003). (ii) Rolling structures (e.g. van den Driessche and Brun, 1987; Marques and Coelho, 2001; Bose and Marques, 2004; Taborda et al., 2004; Marques and Burlini, 2008) – synthetic rotation of muscovite and quartz clasts deduced from drag tails of small calcite grains, mica dust and fluid inclusions, from distortion of halite grains around muscovite and quartz clasts, and from the high angle of many elongated clasts relative to the shear foliation (not observed in the starting material). (iii) σ-Porphyroclast systems (e.g. Passchier and Simpson, 1986; Marques and Coelho, 2001; Bose and Marques, 2004; Taborda et al., 2004; Marques et al., 2005a and b) – stair stepping of tails associated with mica-fish. (iv) Muscovite folding associated with rigid inclusions (rotating or not, Marques and Cobbold, 1995; Rosas et al.,

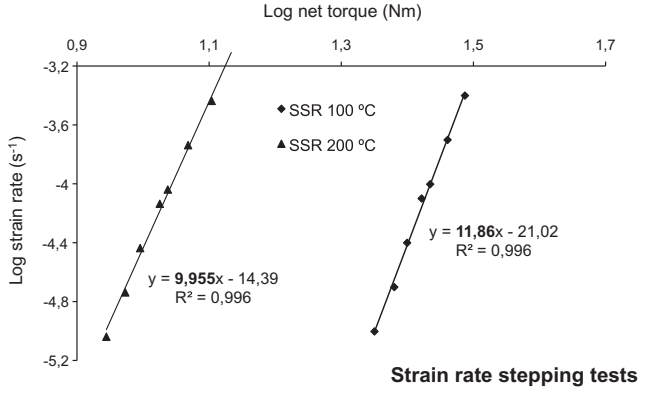

Fig. 3. Strain rate stepping curves used to deduce the stress exponent n. The data are well fit by a power-law curve ($R^2 = 0.996$), with $n \approx 10$ and 12 at 100 and 200 °C, respectively.

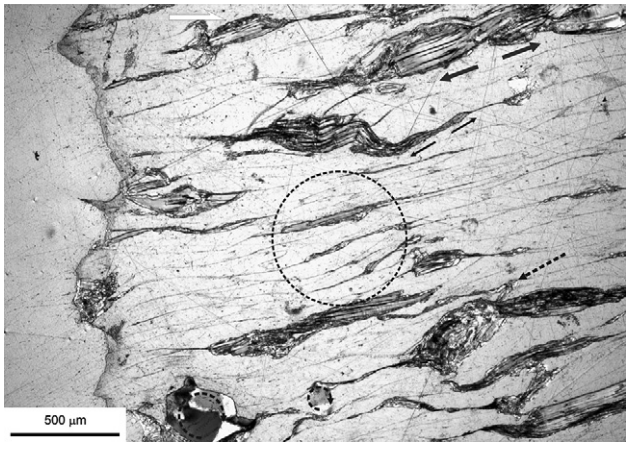

Fig. 4. Transmitted light micrograph image showing general features of sample deformed to $\gamma \approx 5$, at 100 °C, and initial $\varphi = 0°$. Highly stretched halite grains with boundaries marked by (mostly) mica dust and fluid inclusions; boudinage when the mica grain was long and elongated in the extension quadrant (e.g. top center-right); folding when the mica grain was long and elongated in the contraction quadrant (e.g. top center); mica-fish tilted opposite to shear sense and stair stepping tails (e.g. inside dashed circle); mica folding atop a low aspect ratio and strong composite grain (marked by dashed arrow); rotation of rigid quartz grains (bottom left).

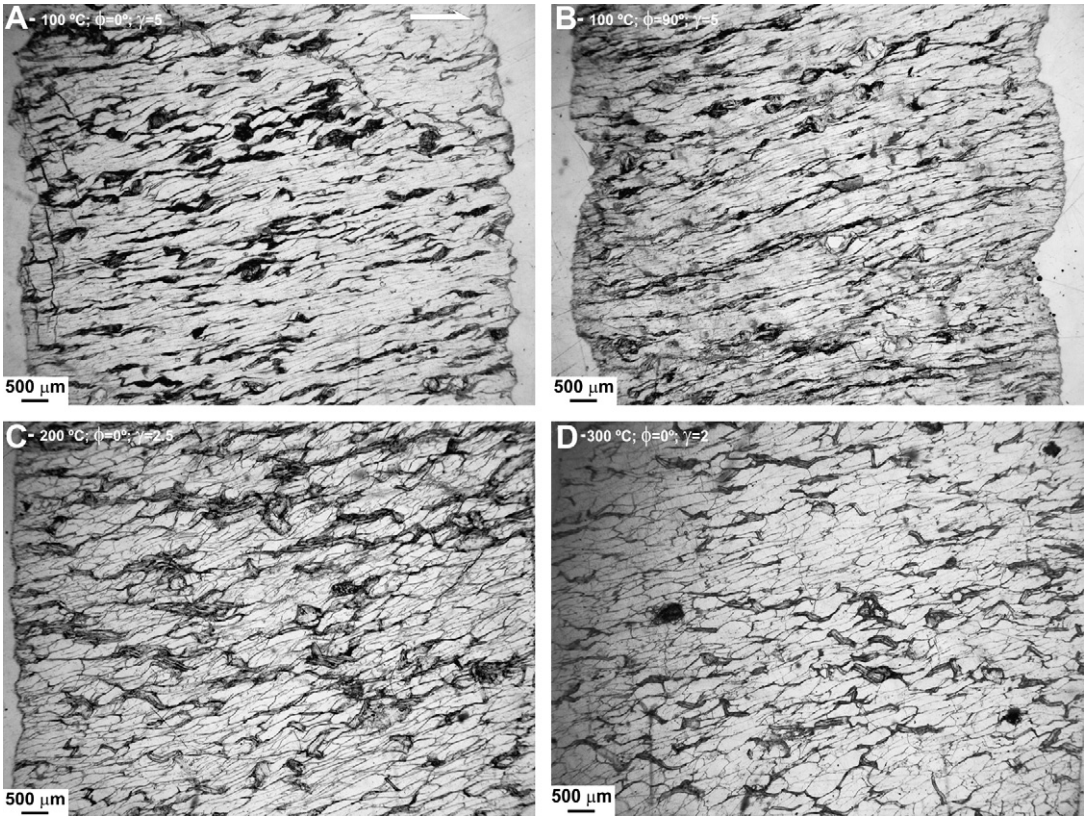

Fig. 5. Transmitted light micrograph image showing rotation and deformational behavior of muscovite flakes with different initial φ, and at different temperature and strain. Note that many mica grains at high angle to the shear plane are typically associated with low strain (C and D), and that folding/kinking is typically associated with initial $\varphi = 0°$ (A, C and D) no matter the temperature. B – Kinking is very rare when initial $\varphi = 90°$. Top to right sense of shear.

2002). (v) Boudins – breaking and separation of muscovite and quartz grains healed by flow of the plastic halite matrix. (vi) Grain size reduction of muscovite by fracturing.

Original folding/kinking could be amplified and flattened because halite in the core of the kinks underwent great plastic flattening. Favorably oriented thin and long muscovite grains folded to an isoclinal geometry, again because of halite behavior.

4. Discussion

The present experiments show that halite deformed plastically in torsion, and muscovite rotated rigidly, or folded/kinked or fractured. We could not find evidence for plastic deformation of the muscovite grains besides slip on {001} cleavage. Therefore we infer that muscovite was stronger than halite under the experimental conditions. Plastically deforming halite crystals had to contour the strong muscovite clasts and were dragged along with their synthetic rotation.

The experimental results raise several questions:

1. Why was the composite aggregate stronger than the single-phase halite aggregate?

The percolation theory considers that the behavior of a two-phase aggregate is dominated by the phase that is connected (insulator/conductor analogy) (e.g. Stauffer and Aharony, 1992; Gueguen and Palciauskas, 1994, for a review of the percolation theory). However, although the mica did not show connectivity (no percolation), the strength of the specimens in the present experiments was greatly influenced by the presence of mica. Therefore other explanations must be sought. Einstein (1906) showed that the viscosity of a fluid increases with the amount of suspended rigid inclusions, which could be an explanation for the increase in strength in the two-phase aggregate. Comparing experimental results with mathematical models, Rybacki et al. (2003) concluded that the strengthening of a soft plastic matrix (in their experiments calcite with dispersed quartz) can occur on a finer scale than the grain scale. They suggested that strengthening may be related to the reduced mobility of dislocations through diffusion of silicon into dislocation cores. The present study does not allow verification if this process happened. Besides the well-known effect of rigid inclusions on the viscosity of a suspension, what we could observe was that: (i) the strong muscovite grains hampered free plastic flowage of the soft halite grains, thus increasing strength of the halite matrix; (ii) muscovite dust was present along halite grain boundaries, which can make the aggregate significantly stronger because it hampers halite plastic strain (e.g. Karato, 2008 and references therein).

At 200 °C, the two-phase aggregate was much stronger than the single-phase halite, and the latter reached a constant flow stress much earlier in contrast to the strain hardening of the two-phase aggregate. At this temperature, the shape of the torque/strain curves is no longer that of single-phase halite; we thus infer that temperature played a role in the mechanical behavior of the aggregates and that the shape of the curves at 200 °C reflected muscovite behavior (which made the aggregate stronger). Since we were not able to measure any change in muscovite strength with temperature, we infer that the strength contrast between halite (exponentially weaker with temperature) and muscovite greatly increased with temperature. It seems therefore that the weak resistance of single-phase halite at 200 °C was not matched by softening due to easy internal slip in muscovite or easy intergranular slip.

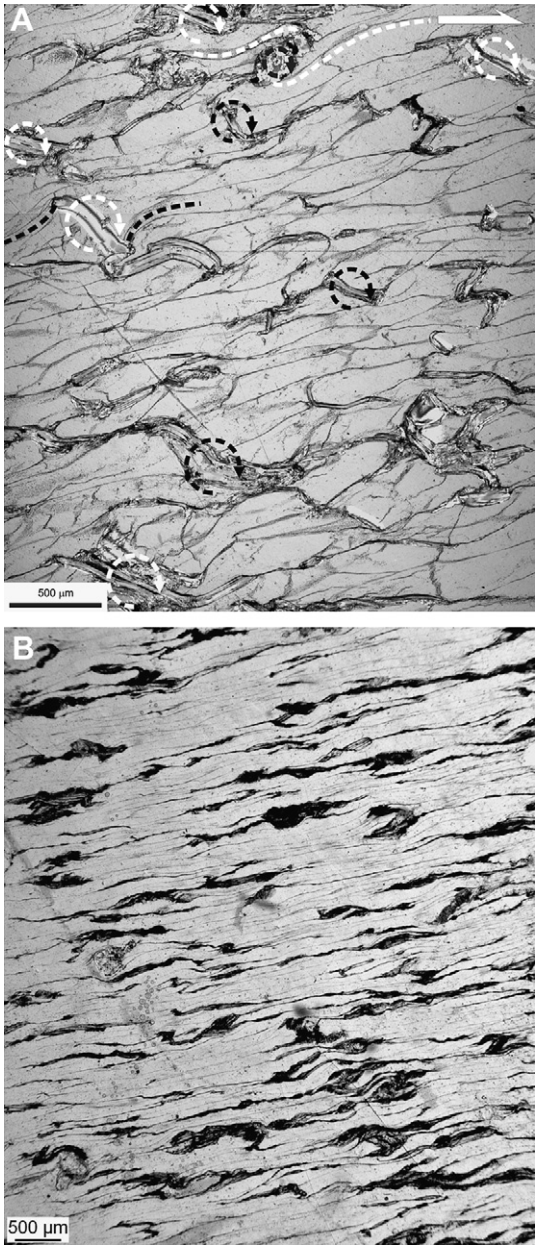

Fig. 6. Transmitted light micrograph image of samples deformed to $\gamma \approx 3$ (A) and $\gamma \approx 6$, with initial $\varphi = 0°$. A – Thick mica porphyroclasts at high angle to the shear plane indicate grain rotation. Also quartz clast at top center with associated drag tails indicates clockwise rotation compatible with applied shear. B – Almost complete absence of mica flakes at high angle to foliation, which is made of halite ribbons (like in stripped quartz mylonites) and aligned muscovite flakes.

The effect of the muscovite clasts on the mechanical properties of the composite aggregate was also reflected on the slope of the torque/strain curves in the very early stages (elastic behavior); higher for the composite aggregates and lower for the single-phase halite. We attribute this increased elastic resistance to the role of muscovite porphyroclasts in strengthening the bulk behavior of the aggregate. Slip along {001} was mostly observed associated with mica folding, and more seldom in grains sub-parallel to applied shear. This means that slip along {001} was not easy and so did not make the aggregate weaker by easy slip along {001}.

2. At 100 °C, why was the $\varphi = 0°$ aggregate the weakest below $\gamma \approx 2.6$ and the strongest above this value?

A possible explanation could be the shape change of the mica megacrysts with strain; more planar at low strains and kinked at higher strains, thus offering greater resistance to halite flow. However, at this stage we do not have enough data to support a better explanation for this behavior.

3. At 200 °C, why was the strength of the aggregate with muscovite and initial $\varphi = 0°$ significantly lower than that of the two-phase aggregate with calcite? Why was the aggregate with muscovite and initial $\varphi = 0°$ weaker than that with $\varphi = 90°$?

Although it seems clear from the experiments that inclusion shape and initial orientation played a role, at this stage we do not have enough data to support an explanation for this behavior.

4. Why was there a large increase in the stress exponent in the composite aggregate in comparison with the single-phase halite aggregate?

Three explanations are possible, and likely complementary: (i) the stress–strain rate relation was affected by the behavior of the strong phase (mica). In fact, if the stress–strain rate relation of (001) slip of muscovite single crystals is fit to a power law, the effective n for muscovite slip is ca. 30 (Mares and Kronenberg, 1993). Therefore, halite–muscovite aggregates had a greater n likely because any deformation of mica would affect the n value of the aggregate. (ii) Given that halite–halite contacts were decorated by mica dust, the inhibition of boundary processes (Karato, 2008) in the plastic deformation of halite could also in part justify the observed large increase in the stress exponent in comparison with pure halite aggregates. (iii) Strong clasts immersed in the halite matrix inhibited free plastic flowage of halite, therefore halite deformation mechanisms were likely affected, with a consequent increase in n. However, with the present experimental results we cannot go further with the explanation for the observed variations in the stress exponent.

5. Why was there clear yielding at 200 °C in comparison to the 100 °C experiments?

A possible explanation is that, at low temperature, the elastic component predominated for longer because the strong muscovite clasts hampered plastic flowage. At 200 °C the elastic component vanished earlier, most probably because at this temperature halite was very weak. Also work hardening at 100 °C was steeper than at 200 °C, which makes the yielding point less conspicuous. We observed that muscovite was strong, but we could not quantify its contribution to the bulk behavior or the difference in muscovite strength at 100 and 200 °C. Anyway, sharp yield points are characteristic of plastic behavior, which suggests that at 200 °C the bulk behavior was more plastic than brittle. Plastic behavior has well defined strain rate sensitivity expressed by the stress exponent of power-law behavior, whereas dry brittle behavior is insensitive to strain rate (e.g. Rutter and Mainprice, 1978). Therefore the stress exponents determined in the present work should reflect the cumulative effect of halite plastic behavior and flow hampering imposed by muscovite clasts.

The present experiments show that a very strong foliation made of halite ribbons and aligned muscovite flakes (shape preferred orientation – SPO) can form before $\gamma = 5$. The present experiments also show that the muscovite flakes rotated towards the shear plane, and fast because they were aligned and sub-parallel to the shear plane before $\gamma = 5$. This was to be expected for an aggregate made of halite (viscous behavior) with immersed strong inclusions (muscovite grains)(e.g. Jeffery, 1922; Ghosh and Ramberg, 1976;

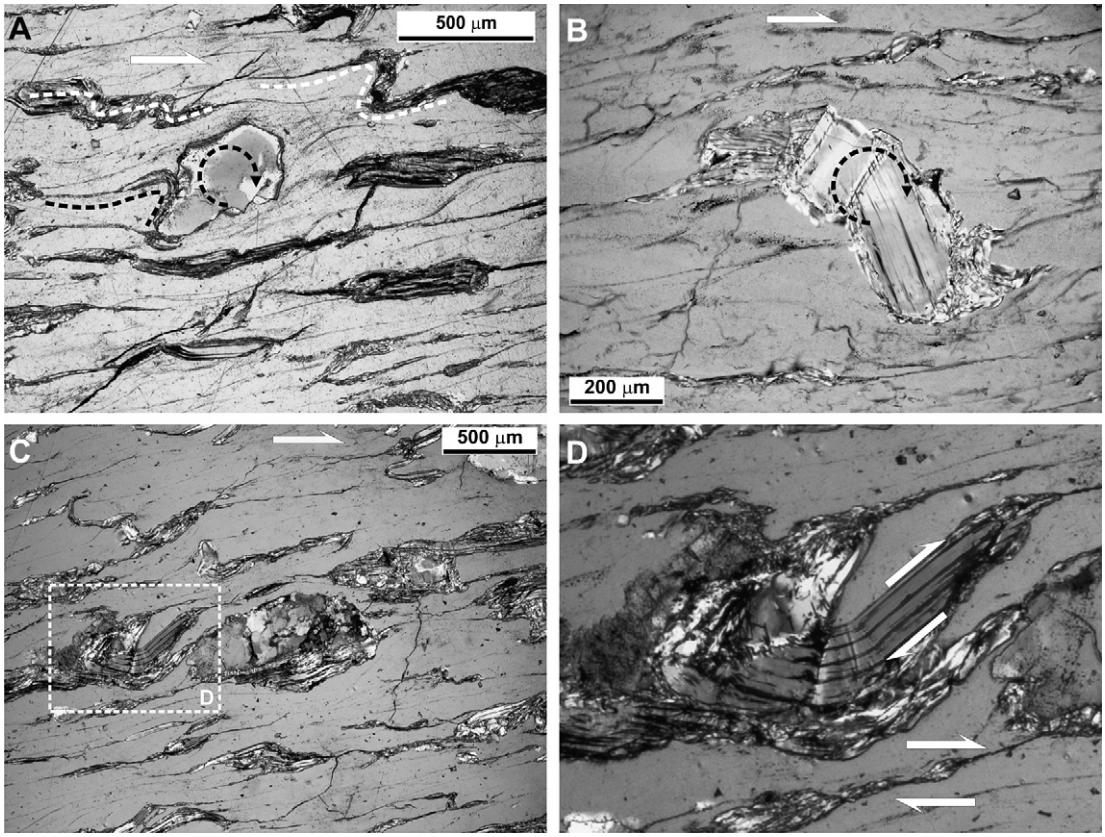

Fig. 7. Transmitted light micrograph image of samples deformed to $\gamma \approx 5$, at 100 °C, and initial $\varphi = 0°$. Note the inhomogeneous character of deformation in the plastic halite matrix, at the grain scale, where halite was plastically stretched and distorted to conform to the more rigid quartz and muscovite clasts. Drag and distortion of tails made of small muscovite grains and distorted halite grains indicate synthetic rotation (marked by arrowed open circles in A and B). Drag tails associated with quartz clast in A indicate that it rotated clockwise by approximately 140°, from an orientation with longest dimension parallel to the applied shear plane. C and D – Mica folding at the rear of rigid quartz clast, very similar to the analogue experimental results of Marques and Cobbold (1995) and Rosas et al. (2002). Fold amplification of muscovite was accommodate by slip along basal cleavage (visible at the right edge of the mica kink zoomed in D) and fold flattening was possible due to strong flattening of halite in the core of the fold. Top to right sense of shear.

Means, 1977; Wilson, 1983; Marques and Coelho, 2003). What the present experiments could not show is whether this muscovite alignment is transient or stable; we needed higher shear strains to check if muscovite grains would continue rotating (transient SPO) or not (stable SPO). A common feature in mica-rich mylonites is the existence of mica-fish, which seems to imply that mica tilting opposite to shear sense is stable. Mica-fish were also common in the present experiments, which can help us constrain the mechanism responsible for the stable orientation of mica flakes. According to Jeffery (1922), all rigid inclusions rotate indefinitely under simple shear; therefore it cannot explain stable orientations. However, it has been shown that (1) associations of pure and simple shears (Ghosh and Ramberg, 1976; Marques and Coelho, 2003), or (2) confinement (e.g. Marques and Cobbold, 1995; Marques and Coelho, 2001; Taborda et al., 2004; Marques et al., 2005a), or (3) slip at the matrix/inclusion interface (e.g. Ildefonse and Mancktelow, 1993; Marques and Coelho, 2001; Mancktelow et al., 2002; Ceriani et al., 2003; Marques and Bose, 2004; Schmid and Podladchikov, 2004; Marques et al., 2005b) can be responsible for a stable SPO. The first hypothesis is ruled out in the present experiments, because there was no axial contraction or extension. The confinement hypothesis can also be ruled out because the walls were far apart (compared to grain size) and there was no rheological layering (stronger layers confining weaker layers). We are therefore left with slip at the mica/halite interface. In nature, a great deal of the mica in mylonites derive from the retrograde breakdown of k-feldspar to quartz + muscovite by addition of water; this means that there were fluids percolating along grain boundaries, which can make interfaces to slip. In the experiments there was no such chemical reaction, but there was a porosity mostly (air) concentrated on grain boundaries, which could trigger slip along mica/halite interfaces.

The present mechanical results in torsion using very soft polymer jackets cannot be compared with previous results using metal jackets, which mask the behavior of halite based aggregates (Marques et al., 2010b). However, we can discuss some results on the relationship between microstructure and strength of the aggregate. Jordan (1987) concluded that the strength of the bulk aggregate decreases as the foliation intensifies. The present experiments do not show such behavior either for composite aggregates with coarse muscovite or for single-phase halite aggregates. Despite the development of a mineral foliation that progressively rotated toward the shear plane in both types of aggregate, the torque/strain curves showed strain hardening, at least to $\gamma \approx 5$. Regarding the microstructure and simple shear experiments, Jordan (1987) also warned that the shear sense could be erroneously deduced from σ- and δ-clasts. In the present experiments we found that all shear criteria were consistent with the applied torsion. However, the shape of muscovite grains seems to have controlled the type of porphyroclast system; rolling-clasts developed mostly from low aspect ratio grains, and σ-clasts developed mostly from high aspect ratio grains. High aspect ratio grains can stay for longer with the longest axis sub-parallel to the shear plane (e.g. Marques and Coelho, 2003) and so be more prone to develop into σ-clasts.

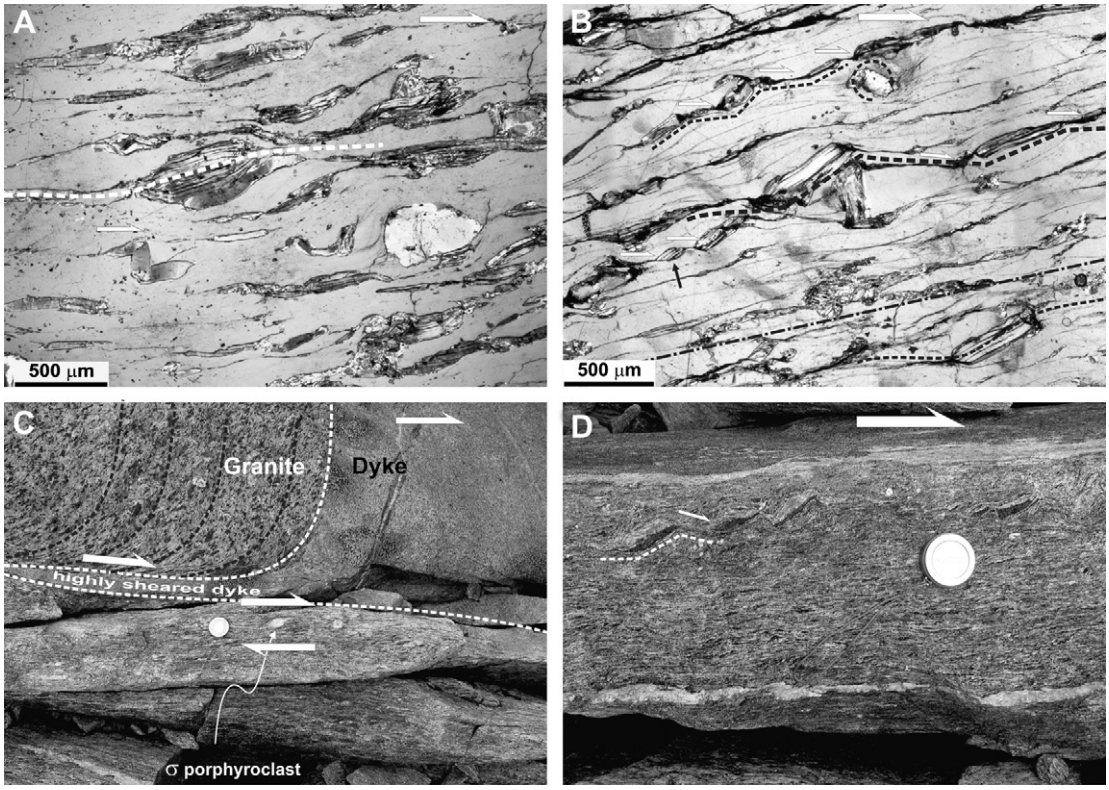

Fig. 8. Comparison of typical experimental microstructures with natural structures in a mylonite from high strain shear zone in the Swiss Alps. Here a meter thick dyke and the host granite were affected by a ductile shear zone at high angle to the dyke, which was sheared and thinned out by the high shear strain. In A note σ mica system very similar to the natural σ feldspar system in C. Also note the similarity of back tilting and associated ductile micro shear bands in B and D.

5. Conclusions

From the results of the present experimental investigation we conclude that:

1. The two-phase aggregate was always much stronger than the pure halite aggregate despite the low volume content of muscovite and absence of connectivity of the strong phase (muscovite).
2. The presence of rigid, rotating inclusions hampered stress relaxation and was responsible for the increased strength and high stress exponents. In both single-phase halite and two-phase aggregates, the stress exponent dropped with temperature, which means that the active deformation mechanisms were essentially temperature sensitive.
3. Shear strain did not localize at the sample scale despite being a two-phase aggregate and having mica.
4. The development of a strong foliation made of halite ribbons and aligned muscovite did not make the composite aggregate weaker than single-phase halite.
5. Inclusion orientation and shape can play a role in the strength of a composite aggregate.
6. SRS tests indicate a power-law viscous behavior of the two-phase aggregate, with a stress exponent $n \approx 12$ or $n \approx 10$ at 100 or 200 °C, respectively, which is significantly lower than the n values determined for aggregates with calcite under similar experimental conditions ($n \approx 19$ or $n \approx 13$ at 100 and 200 °C, respectively).
7. The mechanical data in this study represent actual rheology because we used soft polymers as jackets.
8. The microstructures of the twisted samples are similar to microstructures observed in natural mylonites.

Acknowledgments

The experiments were carried out in the Rock Deformation Lab, ETH-Zürich (ETH 0-12422-97, LZ 3392). F.O.M. acknowledges a sabbatical fellowship by FCT (Portugal) and a guest fellowship by the ETH-Zürich. This is a contribution to research project GEO-MODELS2006 (PTDC/CTE-GIN/66281/2006) rejected by FCT, Portugal.

References

Armann, M., 2008. Microstructural and Textural Development in Synthetic Rocksalt Deformed in Torsion. PhD Thesis, ETH-Zürich, Switzerland.
Barnhoorn, A., Bystricky, M., Kunze, K., Burlini, L., Burg, J.-P., 2005. Strain localisation in bimineralic rocks: experimental deformation of synthetic calcite–anhydrite aggregates. Earth and Planetary Science Letters 240, 748–763.
Berthé, D., Choukroune, P., Jegouzo, P., 1979. Orthogneiss, mylonite and non coaxial deformation of granites: the example of the south Armorican shear zone. Journal of Structural Geology 1, 31–42.
Bloomfield, J.P., Covey-Crump, S.J., 1993. Correlating mechanical data with microstructural observations in deformation experiments on synthetic two-phase aggregates. Journal of Structural Geology 15, 1007–1019.
Bose, S., Marques, F.O., 2004. Controls on the geometry of tails around rigid circular inclusions: insights from analogue modelling in simple shear. Journal of Structural Geology 26, 2145–2156.
Bruhn, D.F., Casey, M., 1997. Texture development in experimentally deformed two-phase aggregates of calcite and anhydrite. Journal of Structural Geology 19, 909–925.
Bruhn, D.F., Olgaard, D.L., Dell'Angelo, L.N., 1999. Evidence for enhanced deformation in two-phase rocks: experiments on the rheology of calcite–anhydrite aggregates. Journal of Geophysical Research 104, 707–724.
Burg, J.-P., Wilson, C.J.L., 1987. Deformation of two phase systems with contrasting rheologies. Tectonophysics 135, 199–205.
Burg, J.-P., Iglesias, M., Laurent, P., Matte, P., Ribeiro, A., 1981. Variscan intra-continental deformation: the Coimbra-Cordoba shear zone (SW Iberian Peninsula). Tectonophysics 78, 161–177.
Ceriani, S., Mancktelow, N.S., Pennacchioni, G., 2003. Analogue modelling of the influence of shape and particle/matrix interface lubrication on the rotational behaviour of rigid particles in simple shear. Journal of Structural Geology 25, 2005–2021.

Choukroune, P., Gapais, D., Merle, O., 1987. Shear criteria and structural symmetry. Journal of Structural Geology 9, 1347–1350.
Delle Piane, C., Wilson, C.J.L., Burlini, L., 2009. Dilatant plasticity in high-strain experiments on calcite–muscovite aggregates. Journal of Structural Geology. doi:10.1016/j.jsg.2009.03.005.
Dresen, G., Evans, B., 1993. Brittle and semibrittle deformation of synthetic marbles composed of two phases. Journal of Geophysical Research 98, 11921–11933.
Dresen, G., Evans, B., Olgaard, D.L., 1998. Effect of quartz inclusions on plastic flow in marble. Geophysical Research Letters 25, 1245–1248.
Einstein, A., 1906. Eine neue bestimmung der moleküldimensionen. Annalen der Physik 19, 289–306, with a correction in 34, p. 591 (1911).
Gaudemer, Y., Tapponnier, P., 1987. Ductile and brittle deformations in the northern Snake Range, Nevada. Journal of Structural Geology 9, 159–180.
Ghosh, S.K., Ramberg, H., 1976. Reorientation of inclusions by combination of pure and simple shear. Tectonophysics 34, 1–70.
Gueguen, Y., Palciauskas, V., 1994. Introduction to the Physics of Rocks. Princeton University Press.
Handy, M.R., 1990. The solid-state flow of polymineralic rocks. Journal of Geophysical Research 95, 8647–8661.
Hobbs, B.E., Means, W.D., Williams, P.F., 1982. The relationship between foliation and strain: an experimental investigation. Journal of Structural Geology 4, 411–428.
Ildefonse, B., Mancktelow, N.S., 1993. Deformation around rigid particles: the influence of slip at the particle/matrix interface. Tectonophysics 221, 345–359.
Jeffery, G.B., 1922. The motion of ellipsoidal particles immersed in a viscous fluid. Proceedings of the Royal Society of London A 102, 161–179.
Jordan, P.G., 1987. The deformational behaviour of bimineralic limestone–halite aggregates. Tectonophysics 135, 185–197.
Kanagawa, K., 1991. Change in dominant mechanisms for phyllosilicate preferred orientation during cleavage development in the Kitakami slates of NE Japan. Journal of Structural Geology 13, 927–943.
Karato, S.-I., 2008. Deformation of Earth Materials: An Introduction to the Rheology of the Solid Earth. Cambridge University Press, New York, p. 463.
Kawamoto, E., Shimamoto, T., 1998. The strength profile for bimineralic shear zones: an insight from high-temperature shearing experiments on calcite–halite mixtures. Tectonophysics 295, 1–14.
Lister, G.S., Price, G.P., 1978. Fabric development in a quartz–feldspar mylonite. Tectonophysics 49, 37–78.
Lister, G.S., Snoke, A.W., 1984. S–C mylonites. Journal of Structural Geology 6, 616–638.
Mancktelow, N.S., Arbaret, L., Pennacchioni, G., 2002. Experimental observations on the effect of interface slip on rotation and stabilisation of rigid particles in simple shear and a comparison with natural mylonites. Journal of Structural Geology 24, 567–585.
Mares, V.M., Kronenberg, A.K., 1993. Experimental deformation of muscovite. Journal of Structural Geology 15, 1061–1075.
Marques, F.O., Bose, S., 2004. Influence of a permanent low-friction boundary on rotation and flow in rigid inclusion/viscous matrix systems from an analogue perspective. Tectonophysics 382 (3–4), 229–245.
Marques, F.O., Burlini, L., 2008. Rigid inclusions rotate in geologic materials as shown by torsion experiments. Journal of Structural Geology 30, 1368–1371.
Marques, F.G., Cobbold, P.R., 1995. Development of highly non-cylindrical folds around rigid ellipsoidal inclusions in bulk simple shear regimes: natural examples and experimental modelling. Journal of Structural Geology 17, 589–602.
Marques, F.O., Coelho, S., 2001. Rotation of rigid elliptical cylinders in viscous simple shear flow: analogue experiments. Journal of Structural Geology 23, 609–617.
Marques, F.O., Coelho, S., 2003. 2-D shape preferred orientations of rigid particles in transtensional viscous flow. Journal of Structural Geology 25, 841–854.
Marques, F.O., Taborda, R., Antunes, J., 2005a. 2-D rotation of rigid inclusions in confined bulk simple shear flow: a numerical study. Journal of Structural Geology 27, 2171–2180.
Marques, F.O., Taborda, R., Antunes, J., 2005b. Influence of a low-viscosity layer between rigid inclusion and viscous matrix on inclusion rotation and matrix flow: a numerical study. Tectonophysics 407 (1–2), 101–115.
Marques, F.O., Schmid, D.W., Andersen, T.B., 2007. Applications of inclusion behaviour models to a major shear zone system: the Nordfjord-Sogn Detachment Zone in Western Norway. Journal of Structural Geology 29, 1622–1631.
Marques, F.O., Burlini, L., Burg, J.-P., 2010a. Rheology and microstructure of synthetic halite/calcite porphyritic aggregates in torsion. Journal of Structural Geology 32, 342–349.
Marques, F.O., Burlini, L., Armann, M., 2010b. Technical note on the strength of copper versus polymer jackets in torsion tests on halite up to 300 °C. Tectonophysics 490, 55–59.
Means, W.D., 1977. Experimental contributions to the study of foliations in rocks: a review of research since 1960. Tectonophysics 39, 329–354.
Passchier, C.W., Simpson, C., 1986. Porphyroclast systems as kinematic indicators. Journal of Structural Geology 8, 831–844.
Paterson, M.S., Olgaard, D.L., 2000. Rock deformation tests to large shear strains in torsion. Journal of Structural Geology 22, 1341–1358.
Price, R.H., 1982. Effects of anhydrite and pressure on the mechanical behaviour of synthetic rocksalt. Geophysical Research Letters 9, 1029–1032.
Ramsay, J.G., 1967. Folding and Fracturing of Rocks. McGraw-Hill, New York, p. 568.
Renner, J., Siddiqi, G., Evans, B., 2007. Plastic flow of two-phase marbles. Journal of Geophysical Research 112, B07203. doi:10.1029/2005JB004134.
Rosas, F.M., Marques, F.O., Luz, A., Coelho, S., 2002. Sheath folds formed by drag induced by rotation of rigid inclusions in viscous simple shear flow: nature and experiment. Journal of Structural Geology 24, 45–55.
Ross, J.V., Bauer, S.J., Hansen, F.D., 1987. Textural evolution of synthetic anhydrite–halite mylonites. Tectonophysics 140, 307–326.
Rutter, E., Mainprice, D., 1978. The effect of water on the stress relaxation of faulted and unfaulted sandstone. Pure and Applied Geophysics 111, 634–654.
Rybacki, E., Paterson, M.S., Wirth, R., Dresen, G., 2003. Rheology of calcite–quartz aggregates deformed to large strain in torsion. Journal of Geophysical Research 108, 2089. doi:10.1029/2002JB001833.
Schmid, D.W., Podladchikov, Y.Y., 2004. Are isolated stable rigid clast in shear zones equivalent to voids? Tectonophysics 384, 233–242.
Stauffer, D., Aharony, A., 1992. Introduction to Percolation Theory. Taylor and Francis.
Taborda, R., Antunes, J., Marques, F.O., 2004. 2-D rotation behavior of a rigid ellipse in confined viscous simple shear: numerical experiments using FEM. Tectonophysics 379, 127–137.
ten Grotenhuis, S.M., Trouw, R.A.J., Passchier, C.W., 2003. Evolution of mica fish in mylonitic rocks. Tectonophysics 372, 1–21.
van den Driessche, J., Brun, J.P., 1987. Rolling structures at large shear strains. Journal of Structural Geology 9, 691–704.
Wenk, H.-R., Armann, M., Burlini, L., Kunze, K., Bortolotti, M., 2009. Large strain shearing of halite: experimental and theoretical evidence for dynamic texture changes. Earth and Planetary Science Letters. doi:10.1016/j.epsl.2009.01.036.
Williams, P.F., Means, W.D., Hobbs, B.E., 1977. Development of axial plane slaty cleavage and schistosity in experimental and natural materials. Tectonophysics 42, 139–158.
Wilson, C.J.L., 1983. Foliation and strain development in ice–mica models. In: Etheridge, M., Cox, S. (Eds.), Deformation Processes in Tectonics. Tectonophysics, 92, pp. 93–122.
Xiao, X., Wirth, R., Dresen, G.H., 2002. Diffusion creep of anorthite–quartz aggregates. Journal of Geophysical Research 107 (B11), 2279. doi:10.1029/2001JB000789.